Pharmaceutical Research, Vol. 22, No. 2, February 2005 (© 2005)
DOI: 10.1007/s11095-004-1195-1

Research Paper

Preparation of Microparticles by Micromixers: Characterization of Oil/Water Process and Prediction of Particle Size

Kathrin Schalper,[1,2] Stephan Harnisch,[1] Rainer H. Müller,[2] and Gesine E. Hildebrand[1,3]

Received June 15, 2004; accepted November 8, 2004

Purpose. A descriptive model for microparticle preparation by micromixers was developed to allow prediction of nascent microsphere size and provide a better understanding of a microscale oil/water (O/W) emulsion process.
Methods. Nascent blank microparticles were prepared by an O/W emulsion method using a micromixer. Seven dimensionless groups were derived from the relevant process parameters. A multiple linear regression model was established on an empirical basis to describe the relationship between the key process parameters and the resulting Sauter particle diameter.
Results. The investigated micromixer is particularly suitable for processing of low-viscosity systems. The particle size is mainly controlled by flow velocity. Reynolds number and the viscosity ratio were found to be the most important dimensionless groups regarding the preparation procedure. Particle size was predicted with an accuracy up to 100% applying the empirically derived equations.
Conclusions. An O/W process using micromixers for microparticle preparation with a multitude of influencing parameters was successfully characterized by application of dimensional analysis. Dimensionless groups turned out to be suitable for prediction of microparticle size with high precision.

KEY WORDS: dimensionless groups; microparticles; microfabrication; O/W emulsion; particle size; prediction; static mixer.

INTRODUCTION

The large and growing variety of pharmaceuticals on the market and in development requires versatile delivery systems that can adapt to the needs of particular applications, especially the capacity to generate a specified delivery rate. Thus, poly (lactide-*co*-glycolide) (PLGA) microparticles have increasingly been applied for the controlled delivery of drugs with different physical and chemical properties (1).

The oil/water (O/W) emulsion/solvent evaporation method is a common technique for preparation of polymeric microparticles (2,3). The basic preparation process involves the emulsification of a polymer dissolved in a volatile solvent into an aqueous surfactant solution. The active substance to be encapsulated is also dissolved or dispersed in the solvent phase. In a second step, the solvent is eliminated using, for example, vacuum evaporation or cross-flow extraction, resulting in the formation of solid particles (4). For encapsulation of hydrophilic molecules, such as proteins and peptides, the water/oil/water (W/O/W) emulsion method was developed (5). Thereby, a primary water/oil (W/O) emulsion containing the active ingredient in the disperse phase is emulsified with an aqueous surfactant solution. A W/O/W double emulsion is formed, which is then subject to a solvent elimination process as described above. Within the production of microparticles through emulsion methods, scale-up is always a big obstacle, as most techniques work batchwise (6). Consequently, the transfer from the lab to industrial scale requires cost-extensive and time-consuming process adaptation. Static micromixers, so far mainly used as reactors for very fast chemical reactions and liquid-liquid extraction processes (7–9), represent a versatile possibility to overcome the problems associated with scale-up for production. Micromixers (IMM, Mainz, Germany) are distinguished by a mixing volume below 100 μl at a total size of 1 cm^3 per assembled mixer. Thereby, scaling-up is achieved by "numbering-up." That means simply to multiply the number of micromixers and run them in parallel (10). By connection of two micromixers, also preparation of multiple emulsions is feasible (7).

[1] Schering AG, D-13342 Berlin, Germany.
[2] Department of Pharmaceutics, Biopharmaceutics and Biotechnology, Free University of Berlin; D-12169 Berlin, Germany.
[3] To whom correspondence should be addressed. (e-mail: gesine.hildebrand@schering.de)

ABBREVIATIONS: c_s, surfactant concentration of the aqueous phase; $d_{particle}$, Sauter diameter of nascent microparticles; $d_{channel}$, width of product channel; Oh, Ohnesorge number (dimensionless quotient [viscous forces/inertia driven forces] under simultaneous consideration of the interfacial tension); Re, Reynolds number (dimensionless quotient [inertia driven forces/viscous forces]); v, flow velocity; V_d, volume of the solvent phase (disperse phase in O/W emulsion process); V_t, total volume of formulation; We, Weber number (dimensionless quotient [interface affecting forces/interfacial tension]); γ, interfacial tension; η_d, dynamic viscosity of the solvent phase (disperse phase in O/W emulsion process); η_c, dynamic viscosity of the aqueous phase (continuous phase in O/W emulsion process); $\eta_{product}$, apparent viscosity of nascent microsphere dispersion; ρ_d, density of the solvent phase (disperse phase in O/W emulsion process); ρ_c, density of the aqueous phase (continuous phase in O/W emulsion process); φ, volume-based phase ratio.

Using a continuous flow setup, mixing is achieved by pumping two phases into the micromixer, which is composed of two sets of comb-like intermeshing channels that are responsible for generation of multilamellar liquid layers. These fluid lamellae disintegrate into droplets when discharging the mixing zone via a rectangular outlet channel. The mean residence time of the process good in the mixing zone amounts less than 100 ms (10). A detailed description of the underlying mixing principle is given by Ehrfeld *et al.* (8). The well defined internal microstructure offers a large effective exchange surface for mass and heat transfer, thereby avoiding the heating processes observed with other continuously operated homogenization equipment like high pressure homogenizers or rotor stator systems (7,11–13). That makes them particularly suitable for processing of heat sensitive substances (14). The compact construction of the operation unit additionally provides an opportunity for production automation and aseptic manufacturing (15).

In order to characterize and quantify complex engineering problems, dimensional analysis is often applied in research and development (16). This analytical method involves the conversion of process parameters into a smaller number of dimensionless groups and has been mainly applied for prediction of scale-up processes (17). The development of a quantitative relationship between a target parameter and the respective dimensionless groups provides a possibility to predict the target variable and to elucidate physical interrelationships of a given process. The model equation often serves as a basis for an overall comparison of the investigated system with similar processes in this field and enhances the fundamental understanding of the technical process (17). Dimensional analysis has been used successfully to describe microencapsulation processes with stirred tank reactors (6), static macro mixers (18), and injection methods (19), but it has not been adopted for modeling of microscale processes.

The purpose of the current work was to establish a model for prediction of particle size and elucidate the principles of O/W processes performed with static micromixers. Dimensional analysis was applied to the microsphere preparation procedure, and seven dimensionless groups were derived from the relevant process parameters. In the following, a quantitative correlation between the dimensionless groups and the resulting nascent microparticle diameter was established empirically. Afterwards, additional experiments were performed to validate the derived equations for prediction of particle size. That will minimize experimental effort for future process optimization steps, serve as basis for comparison with further homogenization systems, and provide a better understanding of the basic principles of microscale processes.

MATERIALS AND METHODS

Materials

Resomer RG 858 [poly (D,L-lactic-*co*-glycolic acid 85:15)] and RG 752, 755, 756 polymers [poly (D,L-lactic-*co*-glycolic acid 75:25) of different molecular weight] were purchased from Boehringer Ingelheim (Ingelheim, Germany). Poloxamer 188 (Synperonic F68) was obtained from SERVA (Heidelberg, Germany).

Methods

Determination of Viscosity, Density, and Interfacial Tension

The viscosities of polymer and Poloxamer 188 solutions, respectively, were determined by Ubbelohde capillary viscosimetry (Schott GmbH, Mainz, Germany). The interfacial tension between solvent and aqueous phases was measured with a processor tensiometer K12 (Krüss GmbH, Hamburg, Germany) equipped with a Wilhelmy plate. Density measurements were performed using an oscillation density measuring unit (DMA 55, Chempro Paar, Graz, Austria).

Preparation of Microparticles

Nascent microspheres were prepared by an O/W emulsion method. The experimental setup is shown in Fig. 1. Micromixers of different product channel widths and a mixing element with 40-μm microchannels (IMM, Mainz, Germany) were used for emulsification. The polymer was dissolved in ethyl acetate and homogenized with an excess of an aqueous Poloxamer 188 solution.

All applied solutions were kept at a defined temperature using a temperature-controlled water bath (Lauda GmbH, Königshofen, Germany). The fluids were conveyed into the micromixer by two high pressure liquid chromatography (HPLC) pumps (LaChrom L-7150, Merck-Hitachi, Tokyo, Japan). The size of the nascent microspheres was measured immediately after preparation and no further hardening steps were performed.

Determination of Particle Size

The size of the nascent microparticles was measured using a laser diffractometer (MasterSizer with Software MS 3.01, Malvern Instruments, Malvern, UK). The system was capable of detecting particles in the range from 0.1 to 80 μm. The results are given as Sauter diameter, the mean of the volume based surface distribution.

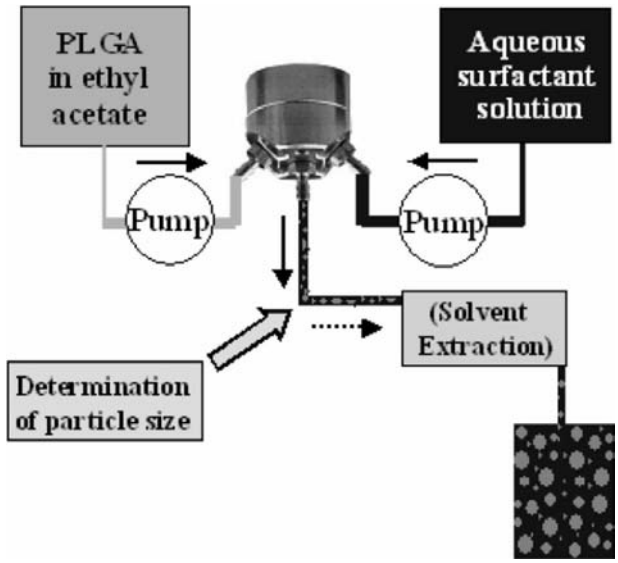

Fig. 1. Experimental setup for microparticle preparation with a micromixer (according to an O/W emulsion method).

Generation of Dimensionless Groups and Experimental Design to Establish Model Equation

In pre-experiments (data not shown), nine relevant independent process parameters were identified, which exert an influence on the target parameter "particle size," expressed as Sauter mean diameter (Eq. 1; see "Abbreviations" footnote above for notation).

$$d_{particle} = f(v, d_{channel}, \eta_d, \eta_c, \rho_d, \rho_c, \gamma, c_s, \varphi) \quad (1)$$

As target parameter, $d_{particle}$, the size of the nascent, nonsolidified particles obtained directly after preparation was chosen. No further hardening steps were performed, as it was aimed to investigate primarily the first process step of a micromixer-based microparticle preparation procedure. The model to be developed should enhance the understanding for the plain microscale process in general and serve as a basis for extension with a second correlation covering the hardening process step currently under conceptualization. The correlation for prediction of nascent microsphere size will be applicable to particles composed of various types of PLGA polymers, since nascent microparticle size was proven to be independent from the type of applied PLGA polymer (pre-experiments, data not shown). Consequently, the hereby established model can be easily supplemented with a second model for prediction of terminal microsphere size by correlating nascent with solid particle size under consideration of polymer concentration and PLGA type related size reduction (18). Recoalesence events after the first process step, leading to failure prediction, are rather unlikely, as Poloxamer 188 was used as stabilizing surfactant. Poloxamer 188 is distinguished by an ultra fast interfacial adsorption kinetics in the range of a few milliseconds (20). For this reason, it is unlikely that the nascent microspheres would undergo significant coalescence over time, even though negligible recoalescence events might occur directly after droplet disruption (21).

The concentration of Poloxamer 188 in the aqueous phase is given in Eq. 1 in two presentations, as interfacial tension γ and percentage concentration c_s. The used surfactant concentrations were above the critical micellation concentration and thus, only slight variations of γ were measured. For that reason a more accessible parameter was added to the relevance list, the surfactant concentration c_s. However, the parameter γ remained included in the relevance list, since it allowed derivation of Ohnesorge number, which is often used for comparison of different homogenization systems (17).

The influencing process parameters ($d_{particle}$, v, $d_{channel}$, η_d, η_c, ρ_d, ρ_c, γ, c_s, φ) were transformed into seven dimensionless groups, using a specific matrix method proposed by Pawlowski (22) (see "Appendix")

$$\Pi_1 = f(\Pi_2, \Pi_3, \Pi_4, \Pi_5, \Pi_6, \Pi_7) \quad (2)$$

The individual dimensionless characteristics are

$$\Pi_1 = \text{target parameter} = \frac{d_{particle}}{d_{channel}} \quad (3)$$

$$\Pi_2 = \frac{\rho_c}{\rho_d} \quad (4)$$

$$\Pi_3 = \frac{\eta_c}{\eta_d} \quad (5)$$

$$\Pi_4 = \varphi \quad (6)$$

$$\Pi_5 = c_s \text{ (given as volume percent)} \quad (7)$$

$$\Pi_6 = \frac{v * d_{channel} * \rho_d}{\eta_d} = \text{Reynolds number [Re]} \quad (8)$$

$$\Pi_7 = \frac{(d_{channel} * \rho_d * \gamma)^{0.5}}{\eta_d} = \frac{\text{Reynolds number [Re]}}{\text{Weber number [We]}^{0.5}} = \frac{1}{\text{Ohnesorge number [Oh]}} = [\text{Oh}]^{-1} \quad (9)$$

The density ratio Π_2 (Eq. 4) showed minor variations over a wide range of polymer and surfactant concentrations (computation not shown) and was not considered for further calculations.The relationship between the target parameter Π_1 and the dimensionless groups can be presented as a power product relationship (Eq. 10).

$$\frac{d_{particle}}{d_{channel}} = a * \left(\frac{\eta_c}{\eta_d}\right)^b * \varphi^c * c_s^{\ d} * Re^e * Oh^{-f} \quad (10)$$

The determination of the coefficients a–f will allow conclusions about the effects of the process parameters on the nascent microsphere size. A total of 68 microsphere batches (prepared in triplicate) grouped in six series was screened in a randomized order to assess the respective coefficient's value (cf. Table I). The blank nascent microspheres were prepared according to the O/W emulsion process mentioned before (cf. "Preparation of Microparticles"). In every series, one process parameter was modified, which led to the variation of the respective dimensionless group(s). The resulting change in

Table I. Investigated Influencing Parameters[a]

Series	Investigated influencing parameter	Modified via	Affected dimensionless group(s)
Ia	v ($\eta_{product} < 1.9$ mPas)	Volume flow	Re (Π_6)
Ib	v ($\eta_{product} > 1.9$ mPas)	Volume flow	Re (Π_6)
IIa	$d_{channel}$ ($\eta_{product} < 1.9$ mPas)	Purpose-built upper mixer housing	Re (Π_6), Oh^{-1} (Π_7)
IIb	$d_{channel}$ ($\eta_{product} > 1.9$ mPas)	Purpose-built upper mixer housing	Re (Π_6), Oh^{-1} (Π_7)
IIIa	η_d ($\eta_{product} < 1.9$ mPas)	Polymer concentration in solvent phase	η_c/η_d (Π_3), Re (Π_6)
IIIb	η_d ($\eta_{product} > 1.9$ mPas)	Polymer concentration in solvent phase	η_c/η_d (Π_3), Re (Π_6)
IV	φ	O/W flow ratio (at constant total flow rate)	φ (Π_4)
V	η_c	Temperature	η_c/η_d (Π_3)
VI	c_s	Surfactant concentration	η_c/η_d (Π_3), c_s (Π_5)

[a] Experimental design used to establish Eqs. 11 and 12 for prediction of particle size.

the target parameter $\prod_1$ was recorded by measuring the size $d_{particle}$ of the nascent microparticles.

In pre-experiments, it was additionally demonstrated that the mixing performance of the micromixer changed, when the apparent viscosity of the nascent microsphere dispersion ("product viscosity") exceeded approximately 1.9–2.0 mPas and larger particle sizes were obtained. Product viscosity is a characteristic, which controls the dispersion performance in a large number of homogenization systems by affecting the nature of shear force transmission within the system (23). Generally speaking, the viscosity of a disperse two-phase system is mainly influenced by the viscosity of the continuous phase and the amount of disperse phase (24). In order to investigate the influence of product viscosity $\eta_{product}$ on the process performance in parallel to the coefficient determination (see Eq. 10), in series I, II, and III $\eta_{product}$ was adjusted to two different values by variation of continuous phase viscosity η_c. Table II summarizes the conditions used to establish a model for prediction of particle size.

No viscosity enhancing agents were used for modification of η_c, as it had been demonstrated in pre-experiments that such additives had led to agglomeration events. Hence, η_c was altered by adding various amounts of surfactant to the aqueous phase. The parameter $\eta_{product}$ was not added to the list of relevant process parameters (cf. Eq. 1), because it is directly linked with two other variables (η_c,, φ), which are already included in the relevance list.

RESULTS AND DISCUSSION

Effect of the Individual Parameter on Particle Size

Parameters Influencing Particle Size via the Differential Pressure Drop

The particle size $d_{particle}$ was mainly controlled by the flow velocity v (Fig. 2) and the width $d_{channel}$ of the product channel (Fig. 3), which both have an impact on the dissipative pressure drop, the pressure difference between infeed and outlet of the mixing zone. The pressure drop corresponds to the energy input in homogenization systems in which volume flow introduces the shear force (e.g., static mixers or microfluidizers). Generally, particle size decreases with increasing pressure drop in suchlike systems (22). As it is shown in Fig. 2, $d_{particle}$ was reduced from 6.6 to 0.6 μm, when *v* was raised from 0.7 to 2.1 m/s. Because v can be adjusted very precisely

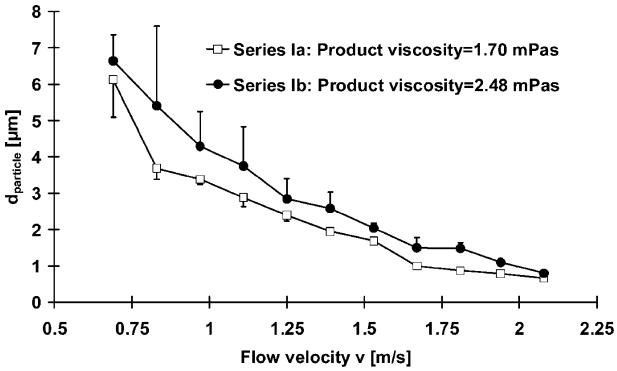

Fig. 2. Effect of flow velocity on particle size. n = 3.

via the volume flow, it is well suitable for control of particle size. Also Freitas *et al.* and Haverkamp *et al.* reported a reduction in particle respectively droplet size by increasing the flow rate (15,25). The maximum *v* generated in the micromixer reached 2.1 m/s (7.5 km/h), a value well below the average observed in static macromixers (26). Thus, the fine degree of dispersion achieved with the micromixer may be mainly due to the small process volume that facilitates homogeneous dissipation of the entire energy input in a volume of less than 20 μl (24). Figure 2 also illustrates the effect of product viscosity $\eta_{product}$ on particle size, in particular when exceeding 1.9 mPas (as discussed in "Generation of Dimensionless Groups"): Working with equal v, the particle diameters of series Ib ($\eta_{product}$ > 1.9 mPas) were up to 60% larger than the diameters of series Ia ($\eta_{product}$ < 1.9 mPas).

The second process parameter directly linked with the dissipative pressure drop in the micromixer is the width of the rectangular product channel $d_{channel}$. An enlargement in $d_{channel}$ generates larger particle sizes, since the dissipative pressure drop decreases. A reduction in $d_{channel}$ by factor 4 resulted in a 3-fold decrease of $d_{particle}$ (Fig. 3). The increase in $d_{particle}$ was more pronounced at batches with higher $\eta_{product}$ (series IIb): Polymer threads were formed, when $d_{channel}$ reached 240 μm. Hence, the respective batch had to be excluded from the analytic considerations. The question is given if $d_{channel}$ actually controls particle size simply by relation with the dissipative pressure drop. Further dispersing mechanisms, for example, laminar elongational flow, may play a role as well. This flow phenomenon is often observed at strong diminutions of the cross-section, for example, at

Table II. Experimental Conditions Applied for Characterization of the O/W Preparation Process[a]

Series	v [m/s]	$d_{channel}$ [μm]	c_s (% (w/w)]	γ^{20} [mN/m]	η_c [mPas]	η_d [mPas]	ρ_d [g/ml]	φ [V_d/V_t]
Ia	0.69–2.08	60	2.0	8.9	1.36	3.52	0.92	0.10
Ib	0.69–2.08	60	4.0	8.9	1.98	3.52	0.92	0.10
IIa	0.52–2.08	60–240	1.0	9.6	1.20	0.96	0.92	0.10
IIb	0.52–2.08	60–240	3.0	9.6	1.67	0.96	0.92	0.10
IIIa	1.67	60	2.0	8.9–16.2	1.36	0.96–29.20	0.91–0.96	0.10
IIIb	1.67	60	4.0	8.9–16.2	1.98	0.96–29.20	0.91–0.96	0.10
IV	1.81	60	2.0	9.3	1.36	2.33	0.92	0.03–0.25
V	1.67	60	2.5	9.3	0.96–2.07	2.20–2.62	0.91–0.92	0.10
VI	1.53	60	0.1–5.0	9.3	1.03–2.26	2.33	0.92	0.10

[a] Experimental conditions employed to establish Eqs. 11 and 12. Equlibrium values of γ were used for calculation, as interfacial equlibrium state in the mixing zone is supposed to be reached within milliseconds (23).

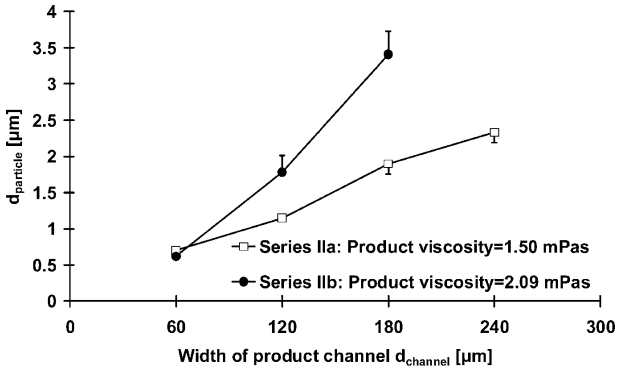

Fig. 3. Influence of product channel width on particle size. n = 3.

high pressure homogenizers with an orifice valve (21). However, the effect of $d_{channel}$ appears to correlate simply with flow velocity *v*, since a smaller $d_{channel}$ does not seem to facilitate the disintegration of the fluid lamellae superproportionally (cf. Figs. 2 and 3). In general, $d_{channel}$ was found to be as effective for variation of particle size as the flow velocity, but the number of commercially available housings with different $d_{channel}$ would be a limiting factor.

Parameters Influencing Particle Size via the Product Viscosity

In mixing systems like static mixers and rotor stator systems, the energy input besides operating properties (like volume flow) is also a function of the physical properties of the material to be processed (23). Concerning the micromixer, the dissipative pressure drop (and thus the energy input) on the one hand is a function of the flow velocity *and* on the other hand it is also determined by $\eta_{product}$. In preexperiments it had been demonstrated that the mixing performance of the micromixer changed, when $\eta_{product}$ exceeded a crucial value (see "Generation of Dimensionless Groups"). The process parameters continuous phase viscosity η_c, surfactant concentration c_s (as the addition of Poloxamer 188 has also an effect on η_c) and phase ratio φ have an immediate influence on $\eta_{product}$, and thus an indirect impact on the dissipative pressure drop as well (24).

The relationship between $d_{particle}$ and η_c is shown in Fig. 4. Raising η_c from 0.96 to 2.07 mPas was followed by an increase in $d_{particle}$ by factor 2. A remarkable increase in $d_{particle}$ could be observed particularly when $\eta_{product}$ reached approximately 1.9 mPas.

A remarkable increase in particle size was also detected when $\eta_{product}$ exceeded a crucial value by modification of φ (cf. Fig. 5, batch containing 25% disperse phase). In contrast, nearly no differences in $d_{particle}$ were observed for batches containing up to 12% disperse phase ($\eta_{product}$ = 1.79 mPas). Karbstein *et al.* mentioned also the possibility of an elevated collision frequency of recently formed droplets by increasing the amount of disperse phase in an emulsion (27). However, nascent microparticles are supposed to be stabilized efficiently with Poloxamer 188 and should show little recoalescence tendency (20).

The range of $d_{particle}$ obtained after modification of c_s is shown in Fig. 6. Concentrations from 0.1% to 1.5% Poloxamer 188 resulted in similar $d_{particle}$ of about 1 µm, which seems to be the marginal dispersity under the investigated conditions. The low emulsifier concentration required may be related to an ultra fast establishment of equilibrium conditions due to the mixing volume in the microliter range and a large surface to volume ratio generated by the micromixer (9). Concentrations above 2.5% led in contrast to an increase in $d_{particle}$. This observation is contradictory to the general assumption that, the higher the surfactant concentration, the finer the degree of dispersion, due to facilitated emulsification and improved stabilization (28). As it is displayed in Fig. 6, the addition of increasing amounts of surfactant elevated simultaneously $\eta_{product}$ and resulted consequently in an altered size of the disperse phase as discussed previously.

Generally speaking, the hereby obtained results demonstrate the specific suitability of the micromixer for low-viscosity systems.

Parameters Influencing Neither Differential Pressure Drop Nor Product Viscosity

The influence of disperse phase viscosity η_d on particle size was pronounced to a minor extent (Fig. 7). Within series IIIa and IIIb, η_d was varied in the range of 1 to 30 mPas, typical for polymer solutions used in microencapsulation processes. An increase of η_d by factor 30 was followed by a just 3-fold increase in $d_{particle}$. Generally speaking, with increasing η_d a liquid requires higher shear forces for disintegration (12). Concerning the micromixer, η_d determines the resistance of the fluid layers against disintegration by the time they enter the product channel. The minor influence of η_d found confirmed the findings by Freitas *et al.* that particle sizes were essentially unaffected by η_d (15). The authors assume that in the case of the micromixer, pumps used for conveyance of the

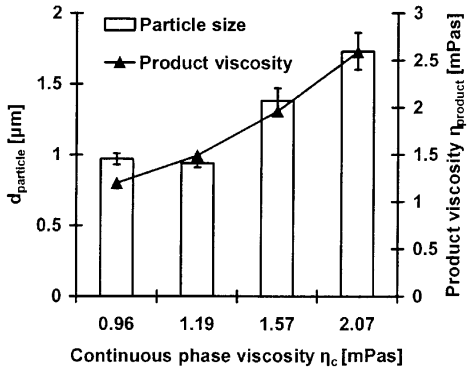

Fig. 4. Effect of continuous phase viscosity on particle size. n = 3.

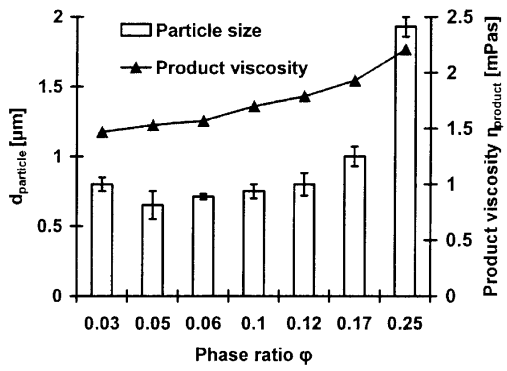

Fig. 5. Impact of phase ratio on particle size. n = 3.

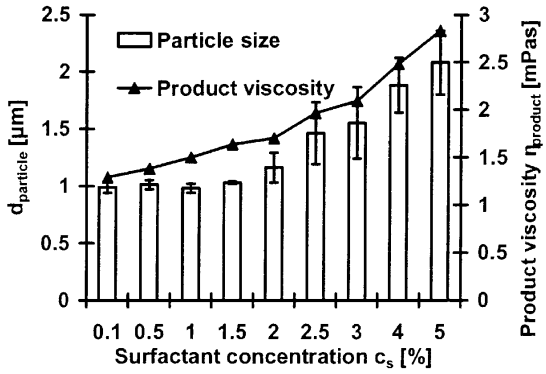

Fig. 6. Particle size as a function of the surfactant concentration. n = 3.

fluids are flow-rate controlled and respond automatically to increased viscosities by increased pressure. Therefore, flow velocity gradients of the fluid lamellae formed in the micromixer remain unchanged and so do the particle sizes. However, in other pressure controlled systems like high pressure homogenizers η_d still has a significant influence on particle size, event though a decrease in homogenization pressure is compensated (11). Potentially, the lamellar structure of the fluid layers in the micromixer facilitates the cutting off of microdroplets, thereby minimizing the effect of η_d.

Dimensional Analysis

In a proximate step the experimental data (cf. Figs. 2–7) were presented using Eq. 10. The coefficients a to f were calculated using a multiple regression method and Eqs. 11 and 12 were derived:

$$\Pi_1 = \frac{d_{particle}}{d_{channbel}} = 16.95 * \left(\frac{\eta_c}{\eta_d}\right)^{0.94} * \varphi^{0.38} * c_s^{-0.05} * Re^{-1.86} * Oh^{-0.65} \qquad \eta_{product} < 1.9 \text{ mPas} \tag{11}$$

$$\Pi_1 = \frac{d_{particle}}{d_{channbel}} = 17.28 * \left(\frac{\eta_c}{\eta_d}\right)^{0.99} * \varphi^{0.71} * c_s^{-0.32} * Re^{-1.95} * Oh^{-0.74} \qquad \eta_{product} > 1.9 \text{ mPas} \tag{12}$$

Two equations were devised to accommodate the different process performance for systems below and above $\eta_{product}$ = 1.9 mPas. In the following the notations for dimensionless groups defined in Eqs. 3–9 will be applied for better readability.

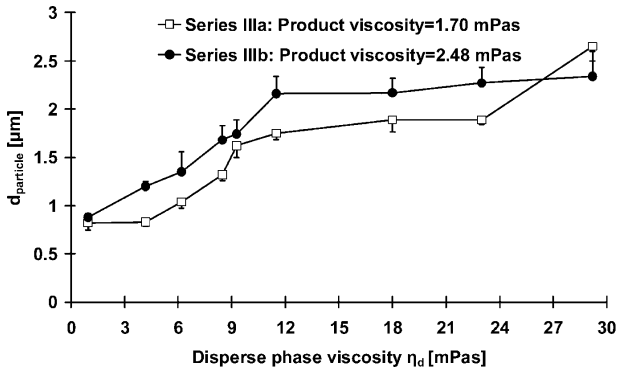

Fig. 7. Influence of disperse phase viscosity on particle size. n = 3.

In Eqs. 11 and 12, Reynolds number [Re] represents the most important dimensionless group with regard to the investigated process. That can be concluded by comparison of the exponents of the individual dimensionless characteristics: A high modulus of an exponent matches a great influence of the corresponding dimensionless figure on the target parameter. The coefficient of [Re] shows clearly the highest modulus and indicates also a reverse proportional dependence of target parameter Π_1 from [Re]. Consequently, the higher the value of [Re], the smaller the value of Π_1, which includes the parameter $d_{particle}$. The overall value of [Re] is in specific determined by v included in this group (cp. Eq. 8), as the other parameters present in [Re] like η_d and $d_{channel}$ show values three to four decimal powers lower than v and the disperse phase density ρ_d vary negligibly (cf. Table II).

Also the viscosity ratio Π_3 has a remarkable bearing on Π_1. The relationship between Π_1 and Π_3 is directly proportional: A high over-all value of Π_3 results in an increase in Π_1 (i.e., in $d_{particle}$). The value of Π_3 is mainly set by the parameter η_c (Eq. 5). Consequently, in Π_3 the importance of the $\eta_{product}$ is reflected again: An increase of η_c leads to a raise of $\eta_{product}$ with its aforementioned implications on $d_{particle}$ (see "Effect of the Individual Parameter on Particle Size").

The Ohnesorge number [Oh] exerts a smaller impact on $d_{particle}$ than [Re], as it can be seen in Eqs. 11 and 12. This difference is certainly related to the presence of v in [Re]. The value of [Oh] is in specific determined by $d_{channel}$. The functional relationship of [Oh] and Π_1 is reverse proportional: A reduction in [Oh] implicates a decrease in $d_{particle}$. Even if none of the factors included in [Oh] exerts a direct effect on $\eta_{product}$, the extent of influence of [Oh] on $d_{particle}$ is affected by the prevailing $\eta_{product}$. That is reflected by the difference in the associated exponents in Eqs. 11 and 12. As it is illustrated in Fig. 7, the relationship between $d_{particle}$ and η_d, which is included in [Oh], is clearly influenced by $\eta_{product}$. Presumably, $\eta_{product}$ controls the shear force vector acting on the disperse phase and thereby against the resistance of η_d (23).

In contrast, the groups φ and c_s have little influence on $d_{particle}$. The effect of φ is more pronounced in Eq. 12 covering products with $\eta_{product}$ > 1.9 mPas. The surfactant concentration c_s shows nearly no influence on particle size, as the low modulus of the exponents indicates in Eqs. 11 and 12. That confirms the experimental findings discussed prior, that is to say over a broad range of c_s similar $d_{particle}$ were obtained

The huge meaning of [Re] for the O/W process is even more obvious comparing the calculated over-all values of the individual dimensionless groups in Table III: [Re] shows values six times higher than [Oh]. Surprisingly, the values of likewise strong assessed Π_3 are comparably small. The group Π_3 may gain more importance when the values of [Re] and [Oh] decrease. Particle diameters increased suddenly superproportionally when v dropped below 0.8 m/s, as it is shown in series Ia and Ib (Fig. 2). That fact may be related to a growing influence of η_d on $d_{particle}$.

The relationship between the target parameter Π_1 (including the determined $d_{particle}$) and individual dimensionless groups (calculated on the basis of values given in Table II) was plotted in Fig. 8. This chart also shows the range of validity for certain process characteristics. Only three dimensionless groups ([Re], φ and Π_3) were plotted, since it was not possible to vary the other dimensionless figures selectively,

Table III. Values of Individual Dimensionless Groups[a]

Series	$d_{particle}/d_{channel}$ (Π_1) [$*10^{-3}$]	η_d/η_c (Π_3)	φ (Π_4)	c_s (Π_5)	Re (Π_6)	Oh (Π_7)
Ia	5.59–51.86	0.39	0.10	0.02	21.32–63.86	8.81
Ib	6.72–56.19	0.56	0.10	0.04	21.32–63.86	8.81
IIa	4.95–5.39	1.25	0.10	0.01	224.74–234.17	33.55–65.74
IIb	5.28–9.91	1.74	0.10	0.03	227.77–234.17	33.55–57.29
IIIa	7.01–22.43	0.05–1.42	0.10	0.02	6.40–187.84	1.11–33.54
IIIb	7.49–19.27	0.07–2.06	0.10	0.04	6.40–187.84	1.11–33.54
IV	5.51–16.36	0.58	0.03–0.25	0.02	83.97	8.81
V	7.40–14.66	0.44–0.79	0.10	0.025	69.20–81.78	12.13–14.39
VI	8.36–17.66	0.44–0.97	0.10	0.001–0.05	70.98	13.61

[a] Values of the individual dimensionless groups were calculated on basis of process variables given in Table II.

thereby keeping constant the values of the other dimensionless groups: The variation of certain process parameters in these cases always affected various dimensionless groups, as it is illustrated in Table I (series II, III, VI). For presentation of Fig. 8, only the data obtained in series Ia, Ib, IV, and V were used. As it can be seen in Fig. 8, the groups $\prod_3$ and φ show sudden changes in their functional relationship with $\prod_1$. The dimensionless groups $\prod_3$ and φ have in common that the process parameters used for modification (η_c, φ) both have also an impact on $\eta_{product}$ (cf. "Generation of Dimensionless Groups"). [Re] in contrast shows no changes of its functional relationship with $\prod_1$, as [Re] was varied selectively via the parameter "flow velocity" that has no influence on $\eta_{product}$. However, v has the strongest effect on $\prod_1$, as the pronounced decline of the graphs presenting [Re] indicates. Finally, it can be concluded that the observed superproportional increase in $\prod_1$ was clearly related to modified $\eta_{product}$. The dispersion performance of the micromixer changed due to an altered shear force transmission (see "Generation of Dimensionless Groups"). Consecutively, the micromixer is especially suitable for processing of low-viscosity systems. Such formulations are commonly prepared by high pressure homogenizers and microfluidizers under drastic conditions (27). The micromixer allows processing of low-viscosity systems under certainly milder conditions than the mentioned high pressure systems (13,14). In general, the dependence of dispersion performance on product viscosity has been well-documented for a broad range of homogenization systems, for example, for high-pressure homogenizers an optimum viscosity range of 1–200 mPas is given (12).

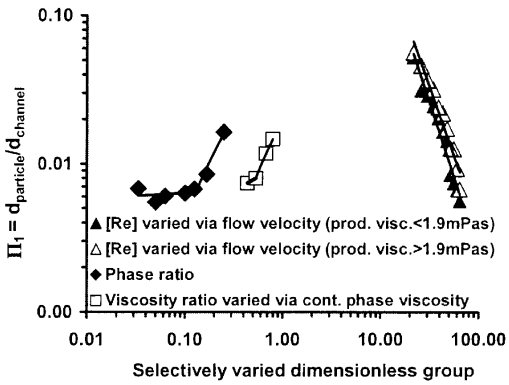

Fig. 8. Influence of dimensionless groups on the target parameter (logarithmic plot). Variations of the slope of the straight lines indicate changes in the functional relationship between the target parameter and the individual dimensionless group (values of dimensionless groups are given in Table III).

Validation of Model Equation

In the following step, Eqs. 11 and 12 were validated for prediction of particle size. Both equations were broken up after the variable $d_{particle}$ to obtain a convenient model for calculation of estimated particle size (Eqs. 13 and 14).

$$d_{particle} = \left\{16.95 * \left(\frac{\eta_c}{\eta_d}\right)^{0.94} * \varphi^{0.38} * c_s^{-0.05} * Re^{-1.86} * Oh^{-0.65}\right\} * d_{channel} \qquad \eta_{product} < 1.9\ \text{mPas} \tag{13}$$

$$d_{particle} = \left\{17.28 * \left(\frac{\eta_c}{\eta_d}\right)^{0.99} * \varphi^{0.71} * c_s^{-0.32} * Re^{-1.95} * Oh^{-0.74}\right\} * d_{channel} \qquad \eta_{product} > 1.9\ \text{mPas} \tag{14}$$

The precision of the prediction was tested by preparing 20 additional batches of microspheres employing random combinations of process parameters. Subsequently, the expected Sauter particle diameter of each batch was calculated using Eqs. 13 and 14 and compared with the experimentally determined particle diameter. Actually measured and predicted particle sizes are summarized in Table IV.

The validation batches showed particle sizes in the range from 0.75 to 4.79 μm. As it can be seen in Fig. 9, particle diameters were predicted with an accuracy up to 100%. In general, batches prepared applying high v or showing low $\eta_{product}$ or η_d, demonstrated the best accordance with the prediction (see column "deviation" in Table IV).

Batches A–L represent batches with $\eta_{product}$ below 1.9 mPas (Table IV). Out of these batches, batch L showed a perfect accordance with the predicted particle diameter. This batch was distinguished by a low $\eta_{product}$ due to the small amount of the disperse phase of 3.3%. Larger deviations were observed mainly with batches showing $\eta_{product}$ above 1.7 mPas (batches G, H, and K) or an elevated γ (batch J).

The batches with product viscosities above 1.9 mPas comprise batches M–T in Table IV. Hereby, especially the particle sizes of batches with lower $\eta_{product}$ were predicted with high accuracy (batches M, P, Q, and S). The deviation between actual and calculated particle diameter ranged between 1% and 8% with regard to these batches. Batches R and T, which are characterized by the highest η_d, showed the largest deviation. The higher dispersion resistance of the dis-

Table IV. Prediction of Particle Size by Means of Dimensionless Groups[a]

Batch	v [m/s]	$d_{channel}$ [μm]	c_s [% w/w]	γ^{20} [mN/m]	η_c [mPas]	η_d [mPas]	ρ_d [g/ml]	φ [V_d/V_t]	$\eta_{product}$ [μm]	$d_{predicted}$ [μm]	$d_{measured}$ [μm]	Deviation [%]
$\eta_{product}$ < 1.9 mPas												
A	1.88	60	2.0	9.6	1.36	0.96	0.92	0.10	1.70	0.65	0.75	12.8
B	1.74	60	1.5	8.9	1.31	2.33	0.92	0.08	1.57	0.84	0.74	13.2
C	1.67	60	1.5	9.6	1.31	2.09	0.92	0.10	1.64	0.97	0.89	9.4
D	0.76	120	0.25	9.6	1.05	9.60	0.92	0.05	1.18	1.60	1.42	12.7
E	0.97	120	1.0	9.3	1.20	2.33	0.92	0.125	1.58	1.9	1.86	4.8
F	0.76	120	0.25	9.6	1.05	2.09	0.92	0.062	1.21	2.16	1.97	9.6
G	1.11	60	1.5	8.9	1.31	2.33	0.92	0.125	1.72	2.29	1.86	23.1
H	0.97	120	2.0	8.9	1.36	3.52	0.92	0.125	1.79	2.35	2.69	12.6
I	0.69	180	2.0	9.6	1.36	0.96	0.92	0.10	1.70	2.36	2.38	0.8
J	1.39	60	1.0	16.2	1.20	11.50	0.91	0.10	1.50	2.42	1.98	22.2
K	0.60	180	1.0	9.6	1.20	0.96	0.92	0.167	1.70	3.41	2.87	18.8
L	0.76	60	2.0	8.9	1.36	18.00	0.93	0.033	1.47	4.79	4.79	0.0
$\eta_{product}$ > 1.9 mPas												
M	1.88	60	2.5	9.6	1.57	0.96	0.92	0.10	1.96	0.77	0.83	7.8
N	1.88	60	3.0	9.6	1.67	2.09	0.92	0.10	2.09	0.81	0.98	20.5
O	1.75	60	4.0	9.3	1.98	2.33	0.92	0.20	2.97	2.18	2.04	6.4
P	1.25	60	2.5	9.3	1.57	2.33	0.92	0.10	1.96	2.28	2.21	3.1
Q	1.11	60	2.5	9.3	1.57	2.33	0.92	0.10	1.96	2.94	2.78	5.4
R	1.74	60	2.5	16.2	1.57	11.50	0.91	0.20	2.36	2.93	3.34	14.0
S	0.97	60	2.5	8.9	1.57	2.33	0.92	0.10	1.96	3.60	3.54	1.7
T	1.74	60	4.0	16.2	1.98	11.50	0.91	0.20	2.97	2.97	3.59	20.9

[a] Experimental conditions used to validate Eqs. 11 and 12. The expected particle diameter $d_{predicted}$ was calculated from the process variables given in this table applying Eqs. 13 and 14.

perse phase made the prediction less reliable, as the standard deviation of batches with η_d above 10 mPas indicates, too (see Fig. 7, series IIIb).

The mean overall deviation in prediction amounted to 11%; 10 of 20 batches showed a deviation of less than 10%. This value can be considered as a very good accordance dealing with such a complex process with nine influencing parameters. Generally, deviations of $d_{particle}$ in the range 1–5% correspond to the approximate reproducibility depending mainly on the applied v and $\eta_{product}$ (cf. Figs. 2 to 7). In addition, the laser diffraction analyzer used for determination of particle size showed within the investigated size range an analytical accuracy of 1.5% to 4% (calibration data not shown), which should be considered for error propagation, too.

In the current study, two equations were established by means of dimensionless groups. These models allow the prediction of nascent microparticle size with high precision under simultaneous consideration of all relevant process parameters. That will help to minimize the number of preexperiments for future process optimization steps and give a better understanding of the dispersion behavior of low-viscosity systems in the microscale range. The physical interrelations, which form the basis of the dispersion process, were elucidated. Performing a small number of experiments, dimensionless groups represented an effective tool to characterize this complex dispersion procedure with a multitude of influencing parameters. The influence of the single process parameters on particle size and interactions were elucidated covering a practice relevant field of activity. The micromixer was shown to be an economic and versatile system for preparation of low viscous disperse systems using mild homogenization conditions.

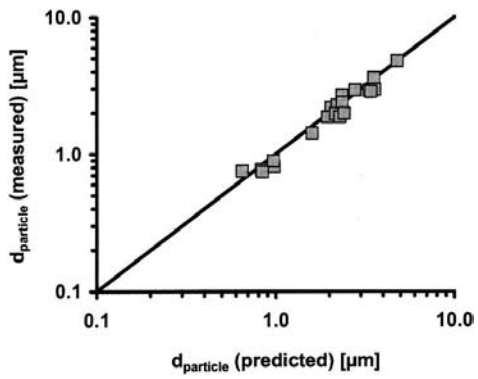

Fig. 9. Correlation between predicted and effectively measured particle diameter (the predicted diameter was calculated according to Eqs. 13 and 14). The straight line corresponds to a concordance of 100% (particle sizes are given in Table IV).

ACKNOWLEDGMENT

This work was supported by a Ph.D. grant of Schering AG, Berlin, Germany.

APPENDIX

Derivation of the Dimensionless Groups

The relevance list required to describe the O/W emulsion process consists of ten parameters (see "Generation of Dimensionless Groups"):

$$\{d_{particle}, d_{channel}, v, \eta_d, \eta_c, \rho_d, \rho_c, \varphi, c_s, \gamma\}$$

A physical relationship between n independent physical quantities can be described by m = n – r independent dimensionless groups, according to Buckingham's theorem (29).

The parameter r represents the rank of the dimensional matrix and is often equal to the number of fundamental dimensions, which are present in the process parameters (here: length L, time T, mass M). In this case, seven linearly independent solutions are set in advance.

$$m = n - r = 10 - 3 = 7$$

The volume-based phase ratio φ and the surfactant concentration c_s are already dimensionless. Two dimensionless characteristics were constituted, the ratios of ($\{\rho_c/\rho_d\}$) and ($\{\eta_c/\eta_d\}$). The three remaining characteristics were derived by application of a special matrix method proposed by Pawlowski (22) and described in detail by Zlokarnik (30).

The dimensional matrix was built using the parameters $d_{particle}$, $d_{channel}$, v, ρ_d, η_d, and γ . The arrangement of the parameters in the dimensional matrix took place in a way that a matrix of unity could be built with as less transformations as possible. Thus, the matrix of unity was reached with four transformations.

		ρ_d	$d_{channel}$	η_d	v	d_p	γ
Mass	M	1	0	1	0	0	1
Length	L	–3	1	–1	1	1	0
Time	T	0	0	–1	–1	0	–2
		core	matrix		residual	matrix	

(A1)

⇓

		ρ_d	$d_{channel}$	η_d	v	d_p	γ	
Mass	M	1	0	0	–1	0	–1	+T
Length	L	0	1	0	–1	1	–1	+3M – 2T
Time	T	0	0	1	1	0	2	–2T
		core	matrix		residual	matrix		

(A2)

In the next step, the dimensionless groups were formed: Each element of the residual matrix formed the numerator of a fraction, whereas the denominator was built of the elements of the core matrix with the exponents listed in the residual matrix.

The following dimensionless groups were derived:

$$\left\{\frac{d_{particle}}{d_{channel}}\right\} = \text{target parameter}$$

$$\left\{\frac{v * d_{channel} * \rho_d}{\eta_d}\right\} = \text{Reynolds number}$$

$$\left\{\frac{d_{channel} * \rho_d * \gamma}{\eta_d}\right\} = \frac{\text{Reynolds number}}{\text{Weber number}^{0.5}} = \text{Ohnesorge number}^{-1}$$

REFERENCES

1. P. B. O'Donnell and J. W. McGinity. Preparation of microspheres by the solvent evaporation technique. *Adv. Drug Del. Rev.* **28**:5–24 (1997).
2. R. Jeyanthi, R. C. Mehta, B. C. Thanoo, and P. P. DeLuca. Effect of processing parameters on the properties of peptide-containing PLGA microspheres. *J. Microencapsul.* **14**:163–174 (1997).
3. A. C. Chang and R. K. Gupta. Stabilization of tetanus toxoid in poly(DL-lactic-co-glycolic acid) microspheres for the controlled release of antigen. *J. Pharm. Sci.* **85**:129–132 (1996).
4. L. R. Beck, D. R. Cowsar, D. H. Lewis, R. J. Cosgrove, C. T. Riddle, S. L. Lowry, and T. A. Epperly. A new long-acting injectable microcapsule system for the administration of progesterone. *Fertil. Steril.* **31**:545–551 (1979).
5. M. Ogawa, H. Yamamoto, T. Okada, T. Yashiki, and T. Shimamoto. A new technique of efficiently entrapped leuprolide acetate into microcapsules of polylactic acid or copoly(lactic/glycolic) acid. *Chem. Pharm. Bull. (Tokyo)* **36**:1095–1103 (1988).
6. Y.-F. Maa and C. Hsu. Microencapsulation reactor scale-up by dimensional analysis. *J. Microencapsul.* **13**:53–66 (1996).
7. H. Löwe and W. Ehrfeld. State-of-the-art in microreaction technology: concepts, manufacturing and applications. *Electrochim. Acta* **44**:3679–3689 (1999).
8. W. Ehrfeld, K. Golbig, V. Hessel, H. Löwe, and T. H. Richter. Characterization of mixing in micromixers by a test reaction: Single mixing units and mixer arrays. *Ind. Eng. Chem. Res.* **38**: 1075–1082 (1999).
9. K. Benz, K.-J. Regenauer, K.-P. Jäckel, J. Schiewe, W. Ehrfeld, H. Löwe, and V. Hessel. Utilization of micromixers for extraction processes. *Chem. Eng. Technol.* **24**:11–17 (2001).
10. V. Hessel, W. Ehrfeld, V. Haverkamp, H. Löwe, and J. Schiewe. Generation of dispersions using multilamination of fluid layers in micromixers. In R. H. Müller and B. H. Böhm (eds.), *Dispersion Techniques for Laboratory and Industrial Scale Processing*, WVG, Stuttgart, 2001, pp. 45–59.
11. P. Goodings. High-pressure homogenization: principles and applications based on EmulsiFlex© equipment. In R. H. Müller and B. H. Böhm (eds.), *Dispersion Techniques for Laboratory and Industrial Scale Processing*, WVG, Stuttgart, 2001, pp. 31–44.
12. S. Schultz, G. Wagner, and J. Ulrich. High pressure homogenization for production of emulsions (German), *Chem.-Ing.-. Tech.* **74**:901–909 (2002).
13. F. Koepsel. *Application of Micromixers in the Preparation of Gas-Filled Microcapsules,* Diploma thesis, University of Dresden, 2002.
14. H. Genth. *Preparation of O/W Emulsions by Micromixers,* Diploma thesis, Technological University of Berlin, 2001.
15. S. Freitas, A. Walz, H. P. Merkle, and B. Gander. Solvent extraction employing a static micromixer: a simple, robust and versatile procedure for the encapsulation of proteins. *J. Microencapsul.* **20**:67–85 (2003).
16. M. Levin. *Pharmaceutical Process Scale Up*, Marcel Dekker, New York, 2002.
17. M. Zlokarnik. Problems in the application of dimensional analysis and scale-up of mixing operations. *Chem. Eng. Sci.* **53**:3023–3030 (1998).
18. Y. F. Maa and C. Hsu. Liquid-liquid emulsification by static mixers for use in microencapsulation. *J. Microencapsul.* **13**:419–433 (1996).
19. B. Amsden. The production of uniformly sized polymer microspheres. *Pharm. Res.* **16**:1140–1143 (1999).
20. R. Miller and K. Lunkenheimer. Adsorption kinetics measurements of some nonionic surfactants. *Coll. Pol. Sci.* **264**:357–362 (1986).
21. S. Brösel and H. Schubert. Investigations on the role of surfactants in mechanical emulsification using a high pressure homogenizer with an orifice valve. *Chem. Eng. Proc.* **38**:533–540 (1999).
22. J. Pawlowski. *The Theory of Similarity in Physical-Technical Research*, Springer-Verlag, Berlin-Heidelberg-New York, 1971.
23. H. Karbstein. *Investigations on the Production and Stabilization of Oil-In-Water Emulsions*, Ph.D. thesis, University of Karlsruhe, 1994.
24. K. D. Danov. On the viscosity of dilute emulsions. *J. Coll. Interface Sci.* **235**:144–149 (2001).
25. V. Haverkamp, W. Ehrfeld, K. Gebauer, V. Hessel, H. Löwe, T. H. Richter, and C. H. Wille. The potential of micromixers for contacting of disperse liquid phases. *Fresenius J. Anal. Chem.* **364**:617–624 (1999).
26. M. Pfeil and R. H. Müller. Static mixing and dispersing of products. In R. H. Müller and B. H. Böhm (eds.), *Dispersion Techniques for Laboratory and Industrial Scale Processing*, WVG, Stuttgart, 2001, pp. 101–110.
27. H. Karbstein and H. Schubert. Developments in the continuous mechanical production of oil-in-water macro-emulsions. *Chem. Eng. Proc.* **34**:205–211 (1995).
28. P. Walstra. Principles of emulsion formation. *Chem. Eng. Sci.* **48**:333–349 (1993).
29. T. Buckingham. On physically similar systems: Illustrations of the use of dimensional analysis. *Phys. Rev.* **4**:345–360 (1914).
30. M. Zlokarnik. Dimensional analysis and scale-up in theory and industrial application. *J. Liposome Res.* **11**:269–307 (2001).